

# High-Efficiency and Stable Emission Wavelength Red InGaN Light-Emitting Diodes with Porous Distributed Bragg Reflectors on Si Substrates

Yi-Sin Cheng, Yen Da Chen, Der-Yuh Lin, Mingbing Zhou, Chih-Ching Cheng, Yi Fu, Hongta Yang,\* and Chia-Feng Lin\*



Cite This: *ACS Appl. Opt. Mater.* 2024, 2, 2241–2247



Read Online

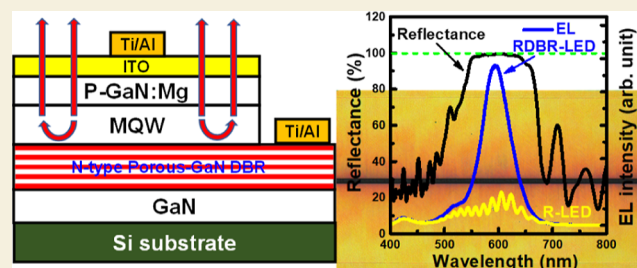
ACCESS |

Metrics & More

Article Recommendations

**ABSTRACT:** Red InGaN light-emitting diodes (LEDs) with porous GaN distributed Bragg reflectors (DBRs) were demonstrated with high directional emission properties, stable emission wavelengths, and prevention of light absorption by the Si substrate. The amounts of peak wavelength that blue-shifted were measured at the values of 18.2 nm for the nontreated red LED and 2.4 nm for the treated red LED with embedded porous GaN DBR structures from a 0.2 to 5.0 mA injection current. The small peak wavelength blue shift, stable emission wavelength, and narrow line width values were shown in the treated red LED due to partially releasing the compressive strain in InGaN active layers by inserting a porous GaN DBR structure. The electroluminescence light emission intensities of the red LED with DBR structures were higher than those of the red LED structures without treatment due to the light reflected by the porous GaN DBR structure and the prevention of light absorption by the Si substrate. From electroluminescence far-field patterns, the divergent angles were reduced from 120 to 85° for the red LED without and with embedded porous GaN DBR structure, respectively. The red LED structures with the embedded porous GaN DBRs consisted of stable emission wavelength, small divergent angles, and narrow line width properties, which have the potential of being used for directional light-emitting sources in micro-LED displays and vertical-cavity surface-emitting laser applications.

**KEYWORDS:** InGaN, red light-emitting diode (LED), porous GaN, distributed Bragg reflectors, Si substrate



## 1. INTRODUCTION

InGaN-based optoelectronic devices have been used for the light-emitting diodes (LEDs), resonant-cavity LEDs,<sup>1–3</sup> and vertical-cavity surface-emitting lasers (VCSELs).<sup>4</sup> Micro-LEDs have been developed for high resolution, high efficiency, and emission wavelength stability and large-size micro-LED displays. The candidate materials for red LEDs are AlInGaP-based and InGaN-based LED structures with similar external quantum efficiencies at small sizes under high current density operation conditions. A significant quantum-confined Stark effect (QCSE)-induced wavelength blue-shift effect is observed in the red InGaN LED with high indium content and large lattice mismatch that was induced by the compress strain effect in InGaN well structures. Many research groups have reported the InGaN-based LED at the red wavelength region.<sup>5–10</sup> The nanorod visible-color-tunable LEDs were grown through the pattern growth on the SiO<sub>2</sub> mask layer.<sup>11</sup> InGaN/GaN tunnel junction nanowires were reported for white LEDs grown on Si substrates.<sup>12</sup> Red InGaN micro-LEDs on silicon substrates have been used for visible light communication applications.<sup>13</sup> InGaN micro-LEDs with blue, green, and red light were

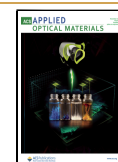
reported on the silicon substrate.<sup>14</sup> Red InGaN micro-LEDs were reported by growing on freestanding GaN<sup>15</sup> and sapphire<sup>16</sup> substrates. The strain relaxation on red LED InGaN/GaN nanowire heterostructures was studied.<sup>17</sup> The embedded distributed Bragg reflector (DBR) structures had been explored, including epitaxial AlGaIn/AlN DBR,<sup>18</sup> epitaxial AlInN/GaN DBR,<sup>19</sup> air-gap/GaN DBR,<sup>20</sup> AlN/GaN epitaxial DBR,<sup>21</sup> and GaN/porous GaN DBR.<sup>22,23</sup> Most of the embedded epitaxial DBR structures serve as reflectors in the resonant-cavity LED and VCSEL devices. Most of the red LED structures had been reported on the AlInGaP-based structure with AlGaAs-based DBR<sup>24</sup> to prevent light absorption by the GaAs substrate. In recent reports, the efficiency of the InGaN-based red LED is still developing and improving at this stage.

Received: July 23, 2024

Revised: October 16, 2024

Accepted: October 21, 2024

Published: October 25, 2024



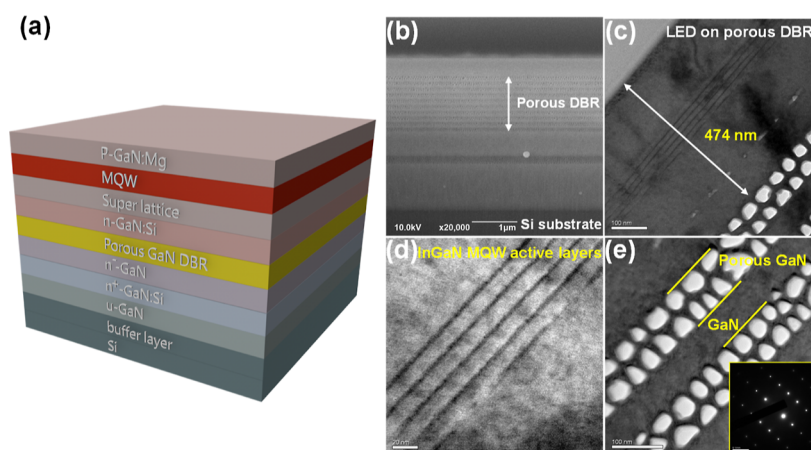


**Figure 1.** (a) Schematic diagram of RDBR-LED structure. (b) SEM micrograph of the RDBR-LED grown on the Si substrate. TEM micrographs of the (c) LED structure above the porous GaN DBR, (d) 5-pair InGaN/GaN MQW active layer, and (e) porous GaN/GaN DBR structures with the TEM diffraction pattern were observed.

The InGaN-based red LED with the embedded DBR structure has been reported to prevent light absorption by the Si substrate and improve the light extraction efficiency. High-efficiency InGaN LED was produced using the pattern sapphire substrate with a sputtering AlN buffer layer. Then, the  $\text{Al}_2\text{O}_3$  substrate can be removed through laser lift-off process using an expensive laser tool. The InGaN LED on the Si substrate can be removed through the wet-etched process without damaging the epitaxial layer of the InGaN LED structure. For the AR/VR micro-LED display applications, the InGaN LED should be bonding on the Si backplate with the driver and circuit. The laser lift-off process makes it hard to remove the sapphire without damaging the Si backplate. After protecting the Si backplate, permission is given to remove the Si substrate through the wet etching process. This study shows that the porous GaN DBR structure acts as an embedded reflector to prevent light absorption on the Si substrate, and partial strain-released layers for the red InGaN-based LED structure were lacking.

This paper demonstrates red InGaN-based LED structures with porous GaN DBRs on Si substrates. By formation of the porous GaN DBR through an electrochemical (EC) etching process, the light emitting from the InGaN active layer has been reflected by inserting a porous GaN DBR structure. The peak wavelengths of electroluminescence (EL) spectra had a small wavelength blue-shifted phenomenon in the treated red LED compared with nontreated red LED structures. High EL intensity and stable emission wavelength of the red InGaN LED were reported in this study by adding embedded porous GaN DBR structures. Optical properties of the red LED structures on Si substrates without and with porous GaN DBR structures were analyzed in detail.

## 2. EXPERIMENTAL DETAILS

Red InGaN LED structures had been grown on the Si(111) substrates by using a metal–organic chemical vapor deposition (MOCVD) reactor. Red LED epi-structures consisted of an AlN buffer layer, AlGaIn/GaN superlattice layers (SLS), the undoped GaN layer, the Si-doped n-GaN ( $n\text{-GaIn:Si}$ ,  $1 \times 10^{19} \text{ cm}^{-3}$ ) layer, the Si-doped n-GaN ( $n\text{-GaIn:Si}$ ,  $1 \times 10^{18} \text{ cm}^{-3}$ ) layer, 10 pairs of  $n^+\text{-GaIn:Si}$  ( $1 \times 10^{19} \text{ cm}^{-3}$ , 85.7 nm)/ $n\text{-GaIn:Si}$  ( $1 \times 10^{18} \text{ cm}^{-3}$ , 66.7 nm) stack structure, InGaIn/GaN SLS, 5 pairs of InGaIn/GaN (3 nm/14 nm) multiple quantum well (MQW) structure, and the p-GaN:Mg (182 nm,  $5 \times 10^{18} \text{ cm}^{-3}$ ) layer. The photolithography process and  $\text{Cl}_2$ -

based inductively coupled plasma reaction ion etching were used to define the trenches of the  $n^+\text{-GaIn:Si}/\text{GaIn:Si}$  stack structure through the dry etching process. The Si-heavy doped GaIn:Si layers in the  $n^+\text{-GaIn:Si}/n\text{-GaIn:Si}$  stack structure were EC-wet-etched as the porous GaIn:Si layers as the porous GaIn:Si/ $n\text{-GaIn:Si}$  DBR structure in a 0.5 M  $\text{HNO}_3$  solution under +8 V bias voltage in room-temperature conditions.<sup>22</sup> A thin indium tin oxide layer (30 nm) was deposited by a sputter deposition process and thermal treatment through a rapid temperature annealing process at 600 °C for 30 s to have conductivity, transparency, and Ohmic contact properties on the p-type GaIn:Mg layer. The Cr/Au metal bilayers were deposited as the metal electrodes by electron-beam evaporation. The mesa region and metal pad size were  $100 \times 100$  and  $70 \times 70 \mu\text{m}^2$ , respectively. The n-type metal pad was deposited on the conductive porous GaIn DBR structure. The nontreated red LED is defined as the R-LED structure. The red LED with the porous GaIn DBR is defined as the RDBR-LED structure. An optical profilometer (Zeta-20) for surface topography and a transmission electron microscope (JEM-2010, JEOL) for cross-sectional TEM micrographs were used. The porosity of the porous GaIn DBR structure was analyzed by using ImageJ open-source software. The reflectance spectra were measured by using an optic spectrometer (USB4000, Ocean Optics). The EL spectra of the LED devices were analyzed using a current source meter (Keithley 236) and a spectrometer (iHR550, HORIBA). A rotation stage system was equipped with a motor controller, scanning from 0 to 180° with a 2° step in the front side of LED chips for far-field radiation patterns of the LED devices.

## 3. RESULTS AND DISCUSSION

In Figure 1a, the schematic diagram of the RDBR-LED structure is shown. The epilayers consisted of the Si substrate, buffer layer, undoped GaIn layer,  $n^+\text{-GaIn:Si}$  layer,  $n^-\text{-GaIn:Si}$  layer, DBR structure,  $n\text{-GaIn:Si}$  layer, InGaIn/GaN SLS, InGaIn/GaN MQW active layer, and p-GaN:Mg layer. In Figure 1b, the EC-etched porous GaIn DBR structure was observed in the RDBR-LED on the Si substrate as seen in the SEM micrograph. The cross-sectional TEM micrographs of the RDBR-LED were observed, as shown in Figure 1c–e. The epitaxial thickness above the bottom porous GaIn DBR was measured at 474 nm, as shown in Figure 1b. In Figure 1c, the micrograph of the five pairs of InGaIn/GaN MQW structure was observed with InGaIn well (3 nm thick) and GaIn barrier (14 nm thick) layers as the stack structure. In Figure 1d, ten pairs of porous GaIn DBR structures consisted of an 85.7 nm thick EC-treated conductive porous GaIn layer and a 66.7 nm thick nonetched GaIn:Si epitaxial layer. The porosity of the

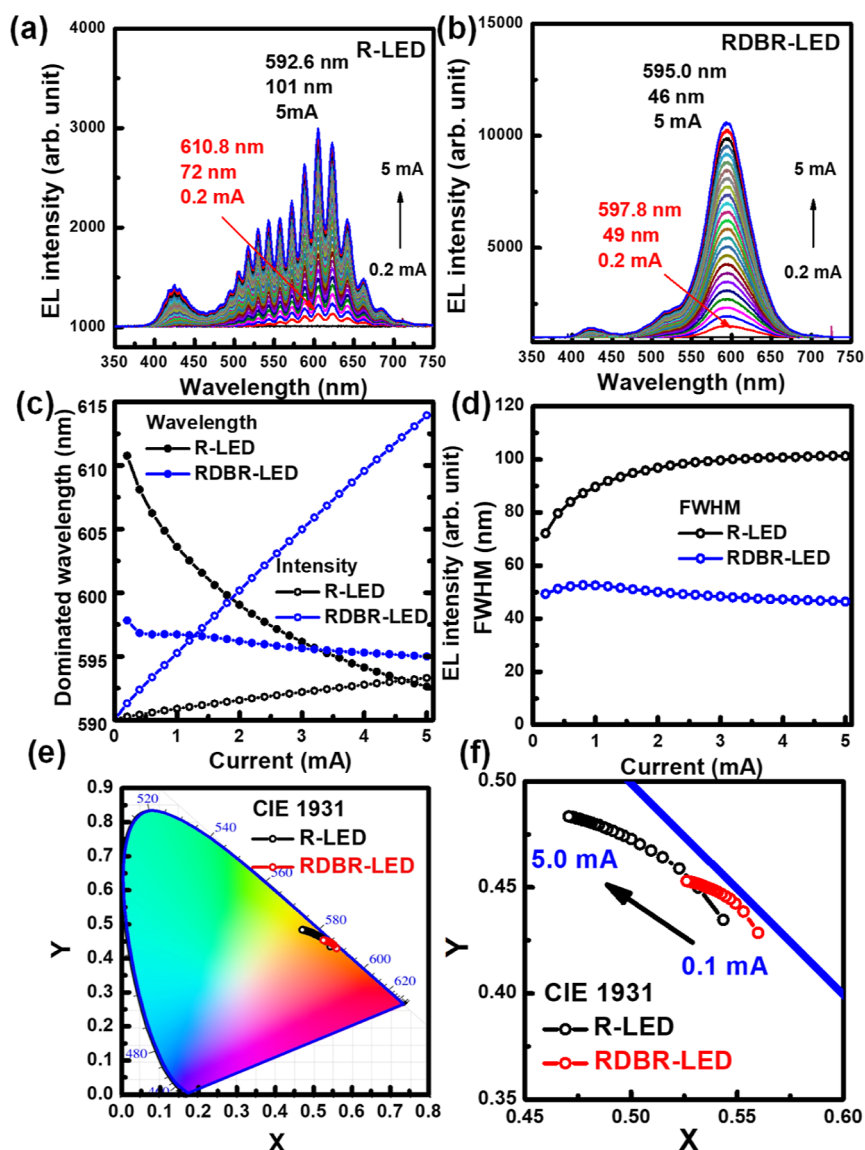


**Figure 2.** EL emission spectra of (a) R-LED and (b) RDBR-LED were measured by varying the injection current from 0.2 to 5 mA, respectively. (c) The dominated peak wavelengths, emission intensities, and (d) fwhm of the R-LED and the RDBR-LED were observed by increasing operation current, respectively. (e,f) The chromatic coordinates ( $x$ ,  $y$ ) in the CIE 1934 converted the EL spectra in both LED structures.

porous layer was calculated at a value of 46% in Figure 1e through ImageJ open-source software.

The EL emission spectra were measured in the R-LED and the RDBR-LED structures, as shown in Figure 2a,b, respectively, by varying the injection current from 0.2 to 5 mA. In Figure 2a, the dominated EL emission wavelength of the R-LED structure was observed at 610.8 nm for the MQW active layer and 425.2 nm for the InGaN/GaN SL layers, at a 0.2 mA injection current. The EL emission spectra with oscillation signals were observed in the R-LED structure due to the optical interference effect between the flat top GaN:Mg/air and bottom AlN/Si interfaces. The dominant emission wavelengths and the full width at half-maximum (fwhm, line width) of the EL spectra were measured at 610.8 nm/72 nm (0.2 mA) and 592.6 nm/101 nm (5 mA), respectively, in the R-LED structure through the curve fitting processes. The weak EL peak at 425.2 nm was emitted from the bottom InGaN SLs, which acted as the strain-released layers. The broad EL emission spectra of the R-LED structure covered the red and

green wavelength range due to larger lattice mismatch at high-indium content InGaN well layers in the active layers. The significant wavelength blue-shifted phenomenon of EL spectra was affected by QCSE, in which the injection carriers have a band-filling effect in the InGaN active layers. In the RDBR-LED structure, the peak EL emission wavelengths and the line widths were measured at 597.8 nm/49 nm (0.2 mA) and 595.0 nm/46 nm (5.0 mA), respectively, as shown in Figure 2b. The blue shift in the EL dominated peak wavelength was due to the combination of the band-filling effect and QCSE for both LEDs. At 5 mA, the peak EL emission intensities of the InGaN active layer at 595.0 nm were higher than those of the InGaN SL at 425.2 nm. The weak EL emission peak at 520 nm was emitted from the bottom InGaN MQW layers with low indium content in the InGaN well layers. In Figure 2b, the dominated EL peak was observed at 600 nm. The smooth EL spectra without oscillation signals were observed in the RDBR-LED compared to the R-LED structure. By formation of the embedded porous GaN DBR structure, the short cavity effect

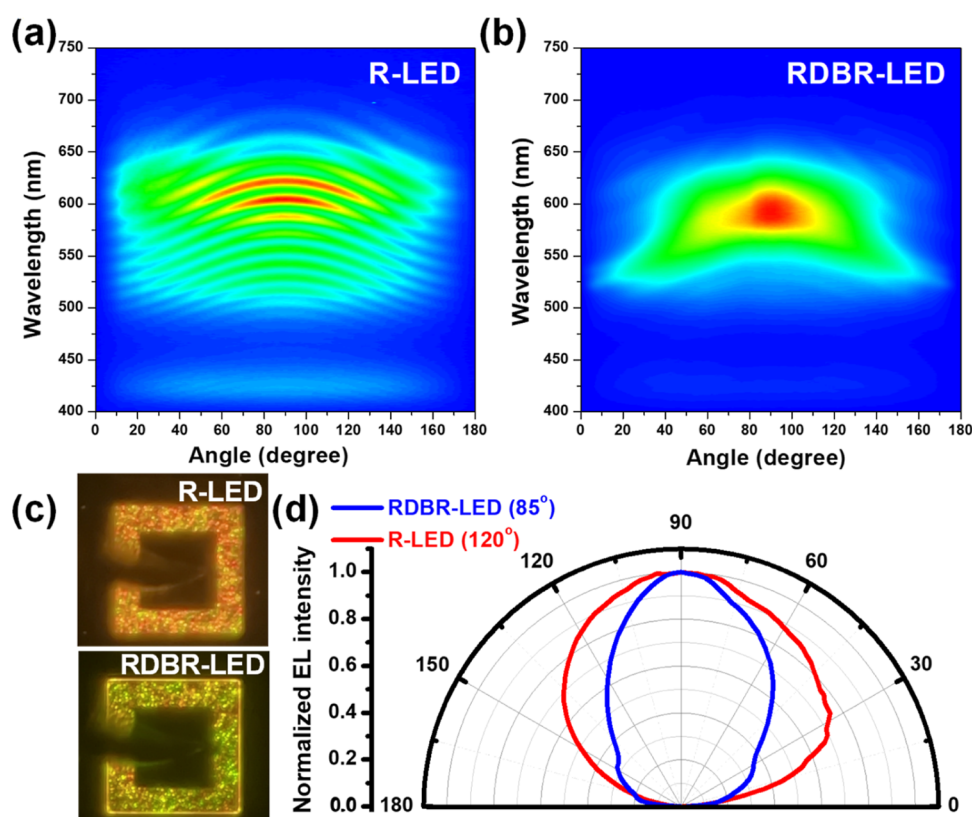


**Figure 3.** Far-field radiative EL spectra of the (a) R-LED and (b) RDBR-LED were measured at 5 mA. (c) The EL emission images of both LEDs were observed at 5 mA. (d) The normalized far-field EL intensity was shown at a 5 mA injection current.

was observed, in which the cavity length was defined between the GaN:Mg/Air interface and the DBR structure. The EL emission intensities of the RDBR-LED structure were higher than those of the R-LED structure. The EL emission light from the InGaN active layer was reflected in the normal direction, and the light absorption in the Si substrate was prevented by inserting the porous GaN reflector. At 0.2 mA, the dominant EL emission wavelengths and fwhm values were blue-shifted from 610.8 nm/72 nm for the R-LED to 597.8 nm/49 nm for the RDBR-LED so that the compress strain in the InGaN active layer was partially released. The fwhm decreasing phenomenon of the RDBR-LED was due to the cavity confinement effect between the top air/GaN:Mg and embedded DBR interfaces. The stable EL emission peak at 595 nm and narrow line width at 46 nm were observed in the RDBR-LED compared with the R-LED.

In Figure 2c, the dominant peak wavelengths and the EL intensity of these LED structures were observed by increasing the injection current. The EL wavelengths of both LED structures were analyzed as the dominant wavelengths through a standard Gaussian fitting model, and the results are shown in Figure 2c,d, respectively. The dominated peak wavelengths had a significant blue-shifted phenomenon in the R-LED structure from 610.8 nm (0.2 mA) to 592.6 nm (5 mA) by adding the injection current. In the RDBR-LED structure, the EL wavelengths had a slight blue-shift phenomenon from 592.6 nm (0.2 mA) to 595.0 nm (5 mA). The amounts of peak wavelength blue-shifted were measured at 18.2 nm for the R-LED and 2.4 nm for the RDBR-LED structures, respectively, from 0.2 to 5.0 mA. The EL light emission intensities of the RDBR-LED structures were higher than that of the R-LED structures due to light reflected by the porous GaN DBR

structure and prevention of light absorption by the Si substrate. In Figure 2d, the fwhm values of EL spectra at 0.2 mA/5 mA injection currents were observed at 72 nm/101 and 49 nm/47 nm for the R-LED and the RDBR-LED structures, respectively. In the EL spectra, the stable emission wavelength and narrow fwhm values were observed in the RDBR-LED as compared to the R-LED structures. That could be caused by the partial strain release in the InGaN active layer by inserting the porous GaN DBR between the MQW active layer and the Si substrate.

We analyzed both LED structures' EL wavelengths, identifying the dominant wavelengths using a standard Gaussian fitting model. The results are presented in Figure 2c. The Gaussian fitting highlights the dominant wavelengths of the EL emission spectra, which should address the reviewer's concerns. Additionally, the typographical errors in the labels of Figure 2c have been corrected in the revised manuscript following the reviewer's suggestion. Furthermore, the chromatic coordinates ( $x$ ,  $y$ ) in the CIE 1934 space were calculated from the EL spectra and are shown in Figure 2e,f for varying operation currents. At 0.1 and 5 mA operation current, the EL emission spectra of both LED structures as shown in Figure 2a,b were calculated as the chromatic coordinates as (0.543, 0.435)/(0.470, 0.484) for the R-LED and (0.560, 0.429)/(0.526, 0.453) for the RDBR-LED, respectively. In Figure 2f, the enlarged figure of Figure 2e shows that the chromatic coordinates are shifted by increasing the injection current. The standard deviation of the chromatic coordinates ( $\pm\Delta x$ ,  $\pm\Delta y$ ) was measured as (−0.073, 0.049) for the R-LED and (−0.034, 0.024) for the RDBR-LED. These results indicate that the color stability of the RDBR-LED, with its porous reflector, is slightly improved compared to that of the R-LED structure.

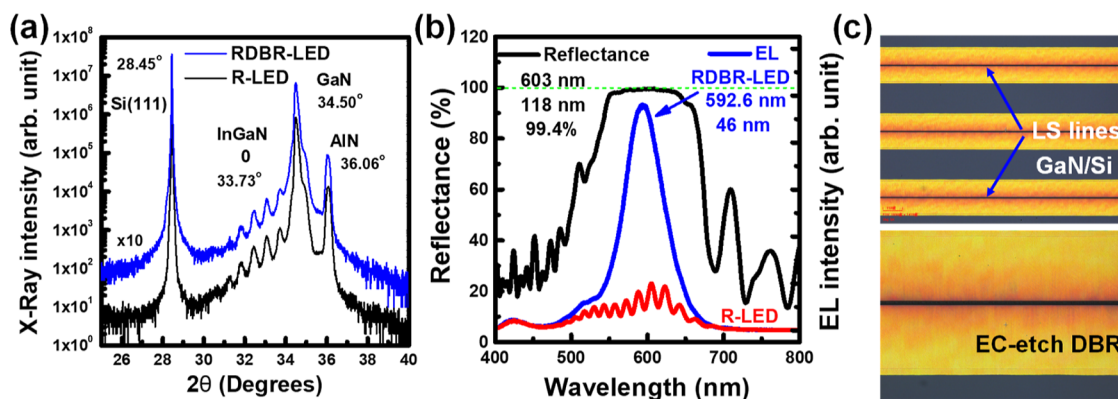


**Figure 4.** (a) The X-ray curves of both LED structures were measured. (b) The reflectance spectrum of the porous GaN DBR structure and EL emission spectra were measured in both LED structures at a 5 mA injection current. (c) LS lines and treated porous GaN DBR regions were observed in OM images.

The far-field EL spectra of LED structures were measured at 5 mA with varying detective angles, in which the normal direction was at  $90^\circ$ , as shown in Figure 3a,b, respectively. In Figure 3a, a high light interference density was observed clearly in the R-LED structure caused by the light interference effect between GaN:Mg/air and AlN/Si interfaces. The EL emission spectra of the R-LED structure covered the red and green wavelength range. In Figure 3b, the dominant EL emission wavelength was about 600 nm with few interference curves for the RDBR-LED structure. The cavity length of the RDBR-LED structure was reduced by the EC-treated DBR structure, and the cavity mode matched the EL emission wavelength at about 600 nm, as shown in Figure 3b.

The EL emission images of LED structures were measured at 5 mA in Figure 3c. The sizes of the mesa region and central metal pad are  $100 \times 100$  and  $70 \times 70 \mu\text{m}^2$  as shown in optical microscopy (OM) images, respectively. The normalized far-field radiative patterns of the EL intensities were measured in both LED structures, as shown in Figure 3d. The divergent angle is defined as the 50% maximum EL intensity angle in the far-field radiation pattern. At a 5 mA operating current, the divergent angles of the EL far-field patterns were reduced from  $120^\circ$  (R-LED) to  $85^\circ$  (RDBR-LED), respectively. Compared to the nontreated R-LED structure, the short cavity length and the narrow divergent angle were observed in the RDBR-LED by adding the porous GaN DBR structure.

In Figure 4a, the X-ray curves were measured for the R-LED and RDBR-LED structures. The peaks of the X-ray curves were measured at  $28.45^\circ$  for Si(111),  $34.50^\circ$  for GaN,  $36.06^\circ$  for AlN, and  $33.73^\circ$  for InGaN epitaxial layers, respectively. The similar X-ray peaks indicated the similar crystalline qualities for the both LED structures. The interference signals of the X-ray curves were observed between Si and GaN diffraction peaks, which indicated the flat interface quality in the InGaN/GaN MQW active layer. From the X-ray curves, the pair thicknesses of the MQW layers were calculated at 17.2 nm for R-LED and 16.5 nm for RDBR-LED. The pair thickness of the InGaN/GaN active layer of RDBR-LED was slightly thinner than that of R-LED structure. This could be due to the partial strain release in the InGaN MQW active layer of the RDBR-LED by incorporating the embedded porous GaN DBR structure. In Figure 2a,b, the EL emission wavelengths had a blue-shifted phenomenon from 610.8 nm for the R-LED to 597.8 nm for the RDBR-LED at a 0.2 mA injection current. The EL peak wavelength blue-shifted phenomenon and the pair thickness

slightly reduced in InGaN MQW active layers were observed in the RDBR-LED, which indicated that the QCSE is slightly reduced compared to the R-LED structure. In Figure 4b, the reflectance spectrum was measured for porous GaN DBR at 603 nm with 99.4% reflectivity and 118 nm stop bandwidth. EL spectra were measured for R-LED and RDBR-LED at a 5 mA operation current. The dominant EL wavelengths were measured at 592.6 nm for the R-LED and 595.0 nm for the RDBR-LED structures, both located within the high reflectivity region of the porous GaN DBR structure. In Figure 4c, the OM images of the EC-etched porous GaN DBR structure were fabricated through the LS process and the lateral wet EC process. The OM images of the treated samples with the device fabricated process were observed from the top view by using microscopy. The EC wet-etching channels were defined and opened at the laser scribing lines. The bottom OM image was observed in large magnification compared with the top OM image. The central dark region between two laser scribing lines is the nontreated region without the embedded porous DBR structure. The red light and dark regions in the OM images were observed for the treated DBR region and the nontreated region with the LED/Si structure, respectively. The red-light region with the EC-treated DBR was formed through a lateral wet-etching process from LS lines. The EL emission properties, crystallinity, and pair thickness of InGaN/GaN active layers of the RDBR-LED structures were affected by forming the embedded porous GaN DBR structure compared to the nontreated R-LED structures. Compared to the nontreated R-LED structure, a high EL intensity was measured in the RDBR-LED with porous DBR structure at normal direction.

#### 4. CONCLUSION

The large compressive strain and prevention of the light absorption phenomenon of the InGaN LEDs on Si substrates with high indium content were solved by inserting a porous GaN DBR layer. A stable EL emission wavelength and a slight blue shift were observed in the RDBR-LED compared to the R-LED, which could be attributed to the partial strain release in the InGaN active layers due to the embedded porous GaN DBR. The light intensities of the RDBR-LED structures were higher than those of the R-LED structures due to the light reflected into the normal direction by the porous GaN DBR structure and the prevention of light absorption by the Si substrate. The divergence angles of the EL intensities were reduced from  $120^\circ$  for the R-LED to  $85^\circ$  for the RDBR-LED.

The stable EL emission wavelength, short cavity length, narrow divergent angle, and high EL intensity at normal direction were demonstrated in the RDBR-LED with the porous GaN DBR structure that can be used for directional light sources, micro-LED display, and VCSEL devices applications.

## AUTHOR INFORMATION

### Corresponding Authors

**Hongta Yang** – Department of Chemical Engineering, National Chung Hsing University, Taichung 40227, Taiwan; [orcid.org/0000-0002-5822-1469](https://orcid.org/0000-0002-5822-1469); Email: [hyang@dragon.nchu.edu.tw](mailto:hyang@dragon.nchu.edu.tw)

**Chia-Feng Lin** – Department of Materials Science and Engineering, National Chung Hsing University, Taichung 402, Taiwan; [orcid.org/0000-0002-1743-4337](https://orcid.org/0000-0002-1743-4337); Email: [cflin@dragon.nchu.edu.tw](mailto:cflin@dragon.nchu.edu.tw)

### Authors

**Yi-Sin Cheng** – Department of Materials Science and Engineering, National Chung Hsing University, Taichung 402, Taiwan

**Yen Da Chen** – Department of Materials Science and Engineering, National Chung Hsing University, Taichung 402, Taiwan

**Der-Yuh Lin** – Department of Electronic Engineering, National Changhua University of Education, Changhua 500, Taiwan; [orcid.org/0000-0001-8525-0655](https://orcid.org/0000-0001-8525-0655)

**Mingbing Zhou** – Latticepower Co., Ltd., Nanchang 330096, China

**Chih-Ching Cheng** – Latticepower Co., Ltd., Nanchang 330096, China

**Yi Fu** – Latticepower Co., Ltd., Nanchang 330096, China

Complete contact information is available at: <https://pubs.acs.org/10.1021/acsaoam.4c00324>

### Notes

The authors declare no competing financial interest.

## ACKNOWLEDGMENTS

The authors gratefully acknowledge the financial support for this research from the National Science and Technology Council (NSTC) under grant nos. MOST 111-2221-E-005-017-MY3, 111-2221-E005-067-MY3, and 112-2811-E-005-012.

## REFERENCES

- (1) Tsai, C.-L.; Lu, Y.-C.; Ko, S.-C. Resonant-Cavity Light-Emitting Diodes (RCLEDs) Made From a Simple Dielectric Coating of Transistor Outline (TO)-Can Packaged InGaN LEDs for Visible Light Communications. *IEEE Trans. Electron Devices* **2016**, *63* (7), 2802–2806.
- (2) Ou, W.; Mei, Y.; Iida, D.; Xu, H.; Xie, M.; Wang, Y.; Ying, L.-Y.; Zhang, B.-P.; Ohkawa, K. InGaN-Based Orange-Red Resonant Cavity Light-Emitting Diodes. *J. Lightwave Technol.* **2022**, *40* (13), 4337–4343.
- (3) Xu, R.-B.; Xu, H.; Mei, Y.; Shi, X.-L.; Ying, L.-Y.; Zheng, Z.-W.; Long, H.; Qiu, Z.-R.; Zhang, B.-P.; Liu, J.-P.; Kuo, H.-C. Emission Dynamics of GaN-Based Blue Resonant-Cavity Light-Emitting Diodes. *J. Lumin.* **2019**, *216*, 116717.
- (4) Hamaguchi, T.; Tanaka, M.; Nakajima, H. A Review on the Latest Progress of Visible GaN-Based VCSELs with Lateral Confinement by Curved Dielectric DBR Reflector and Boron Ion Implantation. *Jpn. J. Appl. Phys.* **2019**, *58* (SC), SC0806.

- (5) Iida, D.; Zhuang, Z.; Kirilenko, P.; Velazquez-Rizo, M.; Najmi, M. A.; Ohkawa, K. 633-nm InGaN-based red LEDs grown on thick underlying GaN layers with reduced in-plane residual stress. *Appl. Phys. Lett.* **2020**, *116* (16), 162101.

- (6) Hwang, J. I.; Hashimoto, R.; Saito, S.; Nunoue, S. Development of InGaN-based red LED grown on (0001) polar surface. *Appl. Phys. Express* **2014**, *7*, 071003.

- (7) Iida, D.; Zhuang, Z.; Kirilenko, P.; Velazquez-Rizo, M.; Ohkawa, K. Demonstration of low forward voltage InGaN-based red LEDs. *Appl. Phys. Express* **2020**, *13*, 031001.

- (8) Zhang, S.; Zhang, J.; Gao, J.; Wang, X.; Zheng, C.; Zhang, M.; Wu, X.; Xu, L.; Ding, J.; Quan, Z.; Jiang, F. Efficient emission of InGaN-based light-emitting diodes: toward orange and red. *Photonics Res.* **2020**, *8*, 1671–1675.

- (9) Pasayat, S. S.; Gupta, C.; Wong, M. S.; Ley, R.; Gordon, M. J.; DenBaars, S. P.; Nakamura, S.; Keller, S.; Mishra, U. K. Demonstration of ultra-small (<10  $\mu\text{m}$ ) 632 nm red InGaN micro-LEDs with useful on-wafer external quantum efficiency (>0.2%) for mini-displays. *Appl. Phys. Express* **2021**, *14*, 011004.

- (10) Lee, D. G.; Choi, Y.; Jung, S.; Kim, Y.; Park, S. Y.; Choi, P.; Yoon, S. High-efficiency InGaN red light-emitting diodes with external quantum efficiency of 10.5% using extended quantum well structure with AlGaIn interlayers. *Appl. Phys. Lett.* **2024**, *124*, 121109.

- (11) Hong, Y. J.; Lee, C.-H.; Yoon, A.; Kim, M.; Seong, H. K.; Chung, H. J.; Sone, C.; Park, Y. J.; Yi, G. C. Visible-Color-Tunable Light-Emitting Diodes. *Adv. Mater.* **2011**, *23*, 3284–3288.

- (12) Sadaf, S. M.; Ra, Y. H.; Nguyen, H. P. T.; Djavid, M.; Mi, Z. Alternating-Current InGaN/GaN Tunnel Junction Nanowire White-Light Emitting Diodes. *Nano Lett.* **2015**, *15* (10), 6696–6701.

- (13) Lu, X.; Li, Y.; Jin, Z.; Zhu, S.; Wang, Z.; Qian, Z.; Fu, Y.; Tu, K.; Guan, H.; Cui, X.; Tian, P. Red InGaN Micro-LEDs on Silicon Substrates: Potential for Multicolor Display and Wavelength Division Multiplexing Visible Light Communication. *J. Lightwave Technol.* **2023**, *41* (16), 5394–5404.

- (14) Zheng, X.; Xu, X.; Tong, C.; Fu, Y.; Zhou, M.; Huang, T.; Lu, Y.; Chen, Z.; Guo, W. Chromatic properties of InGaN-based red, green, and blue micro-LEDs grown on silicon substrate. *Appl. Phys. Lett.* **2024**, *124* (5), 051103.

- (15) Yu, L.; Hao, Z.; Luo, Y.; Sun, C.; Xiong, B.; Han, Y.; Wang, J.; Li, H.; Gan, L.; Jiang, Y.; Chen, H.; Wang, L. Improving performances of ultra-small size (1–20  $\mu\text{m}$ ) InGaN red micro-LEDs by growing on freestanding GaN substrates. *Appl. Phys. Lett.* **2023**, *123* (23), 232106.

- (16) Sanyal, S.; Lin, Q.; Shih, T.; Zhang, S.; Wang, G.; Mukhopadhyay, S.; Vigen, J.; Zhang, W.; Pasayat, S. S.; Gupta, C. Significant reduction in sidewall damage related external quantum efficiency (EQE) drop in red InGaN microLEDs ( $\sim 625$  nm at 1 A  $\text{cm}^{-2}$ ) with device sizes down to 3  $\mu\text{m}$ . *Jpn. J. Appl. Phys.* **2024**, *63*, 030904.

- (17) Malhotra, Y.; Shen, Y.; Wu, Y.; Hanish, J.; Guo, Y.; Xiao, Y.; Sun, K.; Norris, T.; Mi, Z. Impact of Charge Carrier Transfer and Strain Relaxation on Red-Emitting InGaN/GaN Heterostructures. *ACS Photonics* **2023**, *10* (12), 4385–4391.

- (18) Cai, L.-E.; Zhang, B.-P.; Zhang, J.-Y.; Wu, C.-M.; Jiang, F.; Hu, X.-L.; Chen, M.; Wang, Q.-M. Improvement of Efficiency Droop of GaN-Based Light-Emitting Devices by a Rear Nitride Reflector. *Phys. E* **2010**, *43* (1), 289–292.

- (19) Muranaga, W.; Akagi, T.; Fuwa, R.; Yoshida, S.; Ogimoto, J.; Akatsuka, Y.; Iwayama, S.; Takeuchi, T.; Kamiyama, S.; Iwaya, M.; Akasaki, I. GaN-based vertical-cavity surface-emitting Bragg reflectors with graded interfaces. *Jpn. J. Appl. Phys.* **2019**, *58*, SC001.

- (20) Altoukhov, A.; Levrat, J.; Feltin, E.; Carlin, J. F.; Castiglia, A.; Butté, R.; Grandjean, N. High reflectivity air-gap distributed Bragg reflectors realized by wet etching of AlInN sacrificial layers. *Appl. Phys. Lett.* **2009**, *95* (19), 191102.

- (21) Lin, C. F.; Yao, H. H.; Lu, J. W.; Hsieh, Y. L.; Kuo, H. C.; Wang, S. C. Characteristics of stable emission GaN-based resonant-cavity light-emitting diodes. *J. Cryst. Growth* **2004**, *261*, 359–363.

(22) Shiu, G.-Y.; Chen, K.-T.; Fan, F.-H.; Huang, K.-P.; Hsu, W.-J.; Dai, J.-J.; Lai, C.-F.; Lin, C.-F. InGaN Light-Emitting Diodes with an Embedded Nanoporous GaN Distributed Bragg Reflectors. *Sci. Rep.* **2016**, *6* (1), 29138.

(23) Hsieh, T.-H.; Huang, W.-T.; Hong, K.-B.; Lee, T.-Y.; Bai, Y.-H.; Pai, Y.-H.; Tu, C.-C.; Huang, C.-H.; Li, Y.; Kuo, H.-C. Optoelectronic Simulations of InGaN-Based Green Micro-Resonant Cavity Light-Emitting Diodes with Staggered Multiple Quantum Wells. *Crystals* **2023**, *13* (4), 572.

(24) Lee, S. Y.; Moon, J. H.; Moon, Y. T.; Kim, C. S.; Park, S.; Oh, J. T.; Jeong, H. H.; Seong, T. Y.; Amano, H. Improved Light Output of AlGaInP-Based Micro-Light Emitting Diode Using Distributed Bragg Reflector. *IEEE Photonics Technol. Lett.* **2020**, *32* (7), 438–441.